17th World Conference on Earthquake Engineering, 17WCEE

Sendai, Japan - September 13th to 18th 2020

TSUNAMI PROPAGATION PATH FOR THE 1960 VALDIVIA EARTHQUAKE DETERMINED BY SENSITIVITY KERNEL DISTRIBUTIONS

S. Tsuno[(1)], N. Hashimoto[(2)], K. Okamoto[(3)]

[(1)] *Senior Researcher, Railway Technical Research Institute, tsuno.seiji.75@rtri.or.jp*
[(2)] *Researcher, ITOCHU Techno-Solutions Corporation, norihiko.hashimoto@ctc-g.co.jp*
[(3)] *Researcher, National Institute of Advanced Industrial Science and Technology, okamoto.kyosuke@aist.go.jp*

Abstract

To reduce damage of tsunami disaster, it is important to predict an inundation height and an arrival time at the target area by performing a tsunami simulation. To understand the characteristics of tsunami traveling to the target area, it is necessary to elucidate the effect of tsunami propagation path from a tsunami source. The tsunami propagation path has been generally calculated by the wave-ray method. However, the wave-ray method has a difficulty to set appropriate initial and boundary conditions, in contrast to tsunami simulations based on the linear long-wave theory and the shallow water theory. Then, we need to pay attention the characteristics for the results obtained by the wave-ray method. In this study, therefore, by applying the adjoint method to numerical data from a tsunami simulation, we evaluated the tsunami propagation path for the 1960 Valdivia earthauke as a far-field earthquake. This method has a feature to detect tsunami propagation path by calculating cross correlations between tsunami waveforms in the forward direction and waveforms in the reverse direction.

Firstly, we performed the 2-D tsunami simulation to the coast of Japan for the 1960 Valdivia earthauke using the Staggered-Leapfrog method that differentiated the linear long-wave theory. Secondly, we applied the adjoint method to numerical data from the tsunami simulation, to estimate the sensitivity kernel distributions from the coast of Chili to the coast of Japan in the Pacific Ocean. As the results, we obtained the characteristics of the tsunami propagation path for the main phase of tsunami coming from the Hawaiian Islands to the coast of Japan. This result has the same tendency of the result by the wave-ray method in the previous study (Imamura et al., 1990). On the other hand, we obtained the characteristics of the tsunami propagation path for the first arrival of tsunami coming from the south of the Hawaiian Islands to the coast of Japan. Finally, we concluded that this method has a high potential to investigate the characteristic of tsunami propagation path from a tsunami source to the target area.

Keywords: Tsunami propagation path, Adjoint method, Adjoint field, Sensitivity kernel, 1960 Valdivia earthquake

1. Introduction

To reduce damage of tsunami disaster, it is important to predict an inundation height and an arrival time at the target area by performing a tsunami simulation. To understand the characteristics of tsunami traveling to the target area, it is necessary to elucidate the effect of tsunami propagation path from a tsunami source [1]. The tsunami propagation path has been generally calculated by the wave-ray method. However, the wave-ray method has a difficulty to set appropriate initial and boundary conditions, in contrast to tsunami simulations based on the linear long-wave theory and the shallow water theory. Then, we need to pay attention the characteristics for the results obtained by the wave-ray method. In this study, therefore, by applying the the adjoint method [2] to numerical data from a tsunami simulation, we evaluated the tsunami propagation path for the 1960 Valdivia earthauke as a far-field earthquake.

2. Tsunami simulation for the 1960 Valdivia earthquake

2.1 tsunami simulation

Previous studies have already shown that the reproducibility of tsunami simulation for a far-field earthquake can be further improved by taking into account the effects of tsunami dispersibility, Coriolis force [3], and elastic deformation of the seafloor [4] [5]. In this study, however, to calculate a sensitivity kernel in a certain tsunami field and to confirm whether a tsunami propagation path can be appropriately extracted from the sensitivity kernel distribution, we performed a 2-D tsunami simulation using the Staggered-Leapfrog method that differentiated the linear long-wave theory as shown in equation (1), without above effects. The details in the 2-D tsunami simulation for the 1960 Valdivia earthauke is shown in Table 1. The topographical model [6] used in the 2-D tsunami simulation is shown in Fig. 1.

$$\frac{\partial M}{\partial t} = -\frac{gh}{R\cos\varphi}\frac{\partial \eta}{\partial \lambda}, \qquad \frac{\partial N}{\partial t} = -\frac{gh}{R}\frac{\partial \eta}{\partial \varphi}$$
$$\frac{\partial \eta}{\partial t} = -\frac{1}{R\cos\varphi}\left(\frac{\partial M}{\partial \lambda} + \frac{\partial N\cos\varphi}{\partial \varphi}\right) \tag{1}$$

M: longitudinal flow (m^2/s), N: latitudinal flow (m^2/s), η: water level (m), h: water depth (m), g: gravitational acceleration (m/s^2), R: earth radius (m), λ: longitude (deg.), φ: latitude (deg.), t: time (s)

Table 1 – Details used in the 2-D tsunami simulation

Number and size of Grid	Longitudial direction: 1200, Latitudial direction: 780, grid size: 10 arc-minute
Simulation area	East longitude: 100° - 300°, North latitude: -60° - 70°
Topographical model	Bathymetry grid of 1 arc-minute from GEBCO_08 [6]
Time step	10 seconds
Theory	Linear long-wave theory
Initial condition	Slip by Fujii and Satake (2013) [7] Fault parameter by Barrientos and Ward (1990) [8] Crustal deformation by Okada (1992) [9]
Boundary condition	Offshore: Perfectly Matched Layer (Maeda et al., 2016 [10])
	Inshore: Full reflection
Duration of simulation	48 hours after the occurrence of earthquake

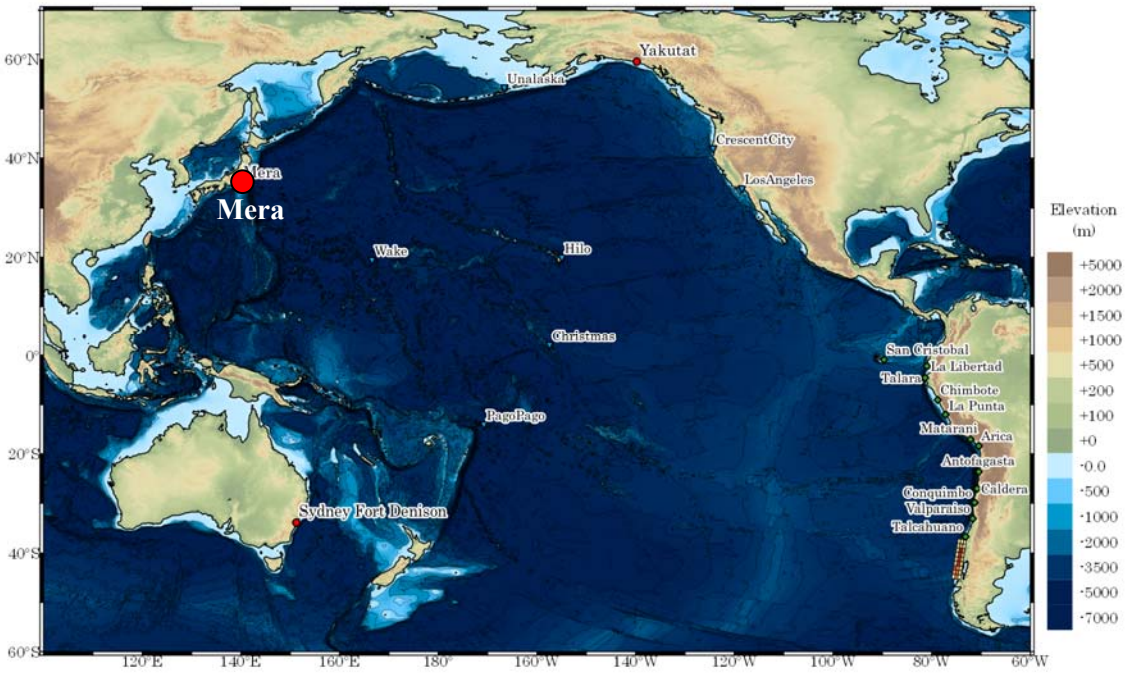

Fig. 1 – Topographical model used in the 2-D tsunami simulation

2.2 1960 Valdivia earthquake

We used slip for each subfault of the 1960 Valdivia earthauke estimated by Fujii and Satake (2013) [7], in the tsunami simulation. Strike, dip and rake of the fault parameters were the same angle of 7.0, 20.0, and 105.0 respectively, for all the subfault [8]. Crustal deformation was calculated by appling the expression of Okada (1992) [9] to the slip distribution for each subfault. The slip and the crustal deformation for the 1960 Valdivia earthauke are shown in Fig.2.

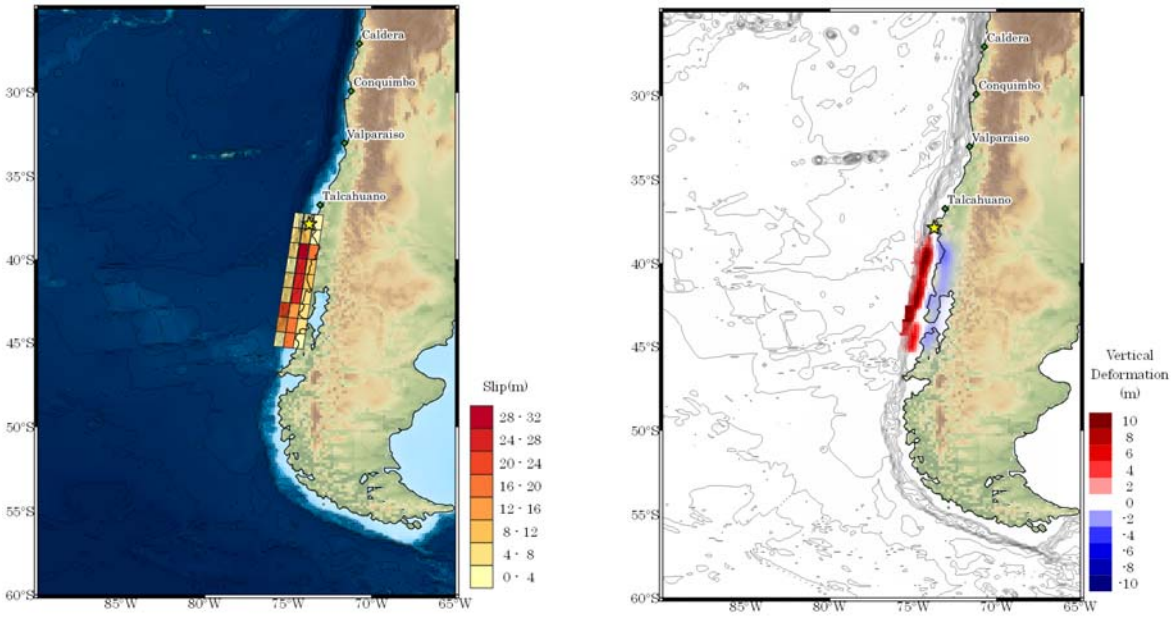

Fig. 2 – Slip (left) and crustal deformation (right) for the 1960 Valdivia earthauke

2.3 Results of tsunami simulation

The distribution of tsunami travel time of the Pacific Ocean by the tsunami simulation and the distribution of the maximum tsunami water level are shown in Fig. 3 and Fig.4, respectively. These results have the similar tendency that the tsunami speed becomes slower and the tsunami water level becomes higher in the Hawaiian Islands and the Johnston Atoll, as shown by Imanura et al. (1990) [1]. Tsunami reaches the coast of Japan in about 22 hours after the occurence of the 1960 Valdivia earthquake.

The tsunami waveforms by the tsunami simulation were compared to the tsunami data (tide gauges) in the coast of South American Continent for the 1960 Valdivia earthauke [7] as shown in Fig. 5. The tsunami waveforms by the tsunami simulation are in the good agreement with the tsunami data (see Fig. 5), which were used to the tsunami inversion of slip distribution on the fault [7].

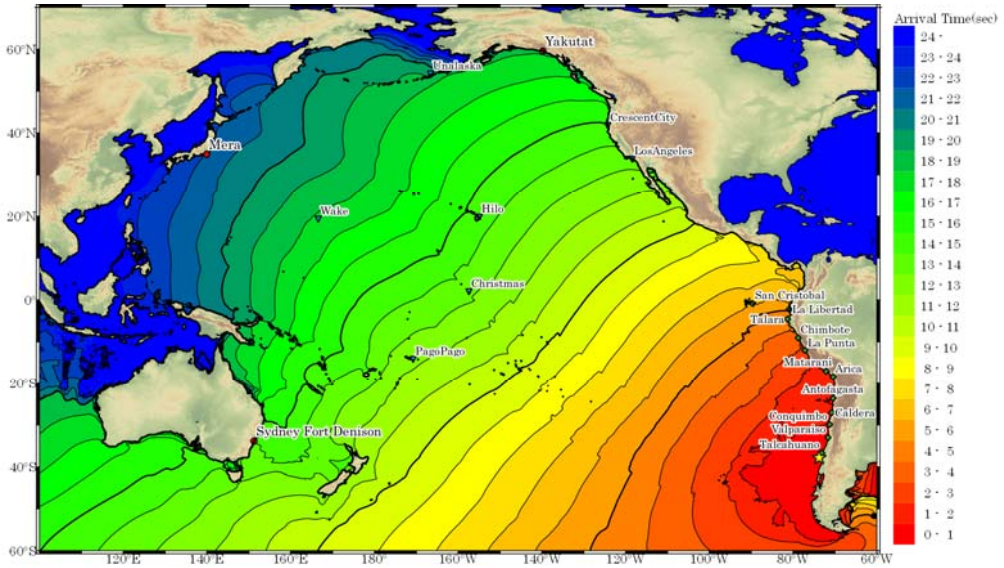

Fig. 3 – Distribution of tsunami travel time in the Pacific Ocean by the tsunami simulation

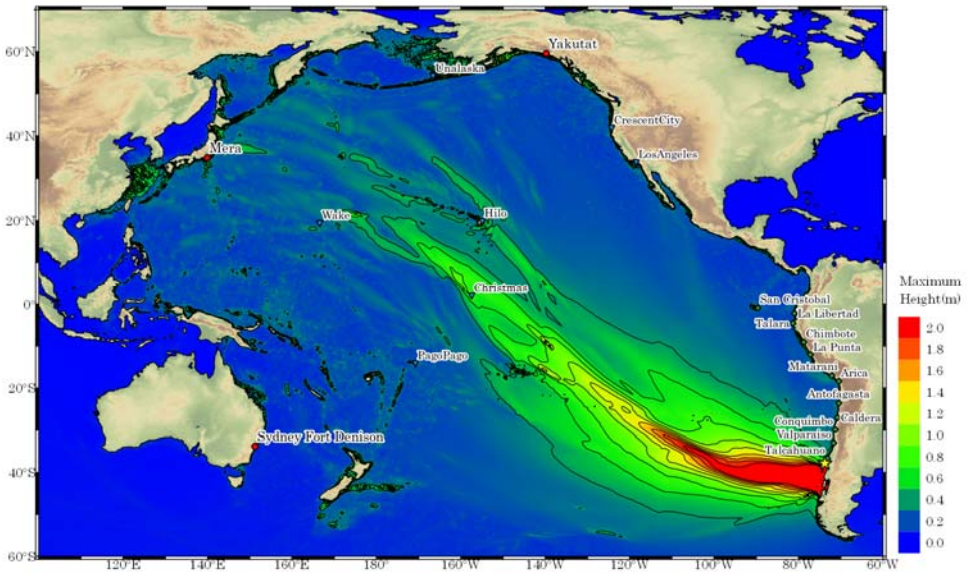

Fig. 4 – Distribution of the maximum tsunami water level in the Pacific Ocean by the tsunami simulation

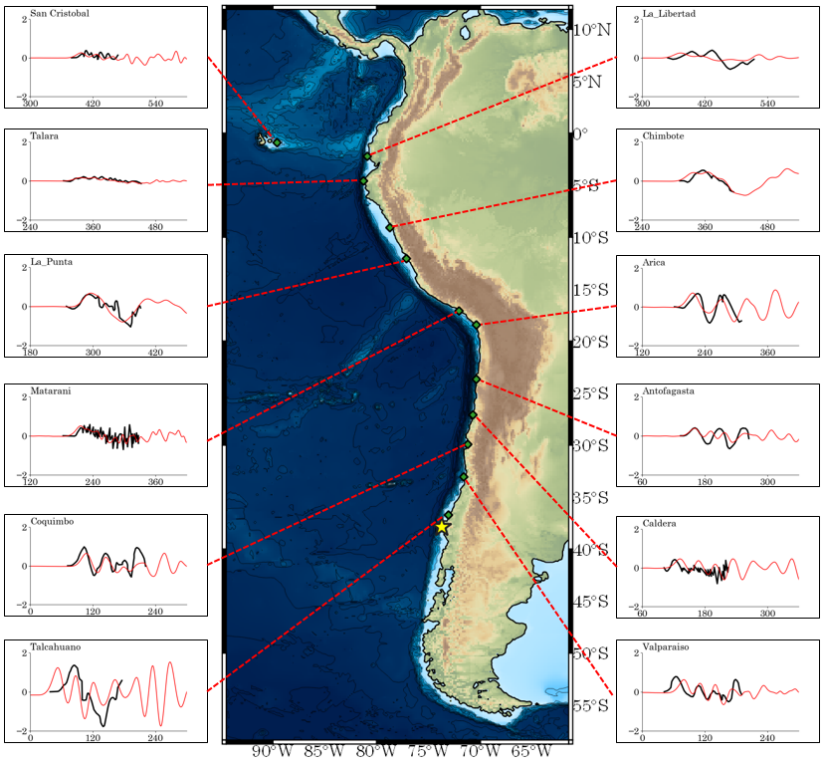

Fig. 5 – Comparison of tsunami waveforms by the tsunami simulation to the tsunami data (tide gauges) [7] in the coast for the 1960 Valdivia earthauke (black line: tsunami data, red line: tsunami simulation)

3. Tsunami propagation path

3.1 Adjoint field and sensitivity kernel

To understand the characteristics of tsunami traveling to the target site, in this study, we applied the adjoint method, which is expressed by the equation of (2) to the numerical data from the 2-D tsunami simulation. Details of adjoint field and sensitivity kernel are described in Tromp et al. (2005) [2].

$$\bar{\eta}(x, x_r, T-t) = \int_0^{T-t} G(x, x_r; T-t) \cdot \eta(x_r, T-t)\, dt \qquad (2)$$

x_r: observation station, T: observation time length (s), G: Green's function, η: tsunami water level (m)

By the equations of the adjoint field and tsunami field, the sensitivity kernel for tsunami waveforms at an observation station can be obtained from the equation of (3).

$$K(x, x_r) = \int_0^{T} \bar{\eta}(x, x_r, T-t) \cdot \partial_t^2 \eta(x, t)\, dt \qquad (3)$$

3.2 Tsunami propagation path

To evaluate the tsunami propagation path from the coast of Chili to the coast of Japan by the adjoint method, we set up the observation point in Mura (Japan), as shown in Fig. 1. As the time length (T in the equation of [2]) for the analysis, we selected a time-window of 1,635 and 1,361 minutes for the main phase, in which the maximum amplitude of tsunami is included and for the first arrival of tsunami produced by the 1960 Valdivia earthquake and propagated in the Pacific Ocean, respectively (Fig. 6 and Fig. 7).

Fig. 8 and Fig.9 show the sensitivity kernels for the main phase and the first arrival of tsunami, respectively. In case of the result for the main phase of tsunami, a various path such as the tsunami reflected from the coast of the Pacific Rim, affects the sensitivity kernel to be slightly distorted (See Fig. 8); however, the sensitivity kernel has the same tendency that the tsunami produced by the 1960 Valdivia earthquake and propagated in the Pacific Ocean from the coast of Chili to the coast of Japan pass the north of the Hawaiian Islands, the Johnston Atoll, and the vicinity of the Line Islands, as shown by Watanabe (1985) [11]. On the other hand, In case of the result for the first arrival of tsunami, the tsunami propagates in the Pacific Ocean, avoiding the path of the southern part of the Hawaiian Islands and the Johnston Atoll, in which the tsunami to the coast of Japan is amplified by the interference effect. The reason is that the first arrival of tsunami propagates in the path of the Pacific Ocean where the tsunami speed is higher, compared to the propagation for the main phase of tsunami.

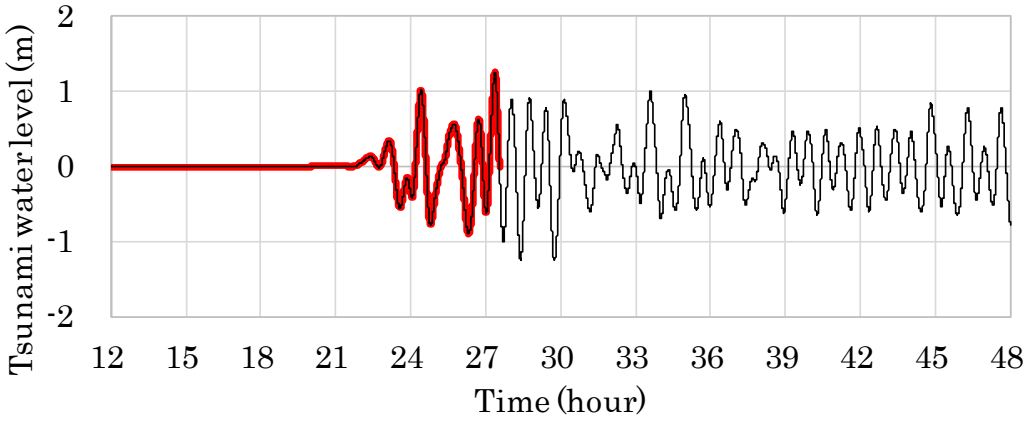

Fig. 6 – Tsunami waveform at Mera, Japan for the 1960 Valdivia earthquake (red line: observation time length [T] of 1,635 minutes after the occurrence of the earthquake including the main phase)

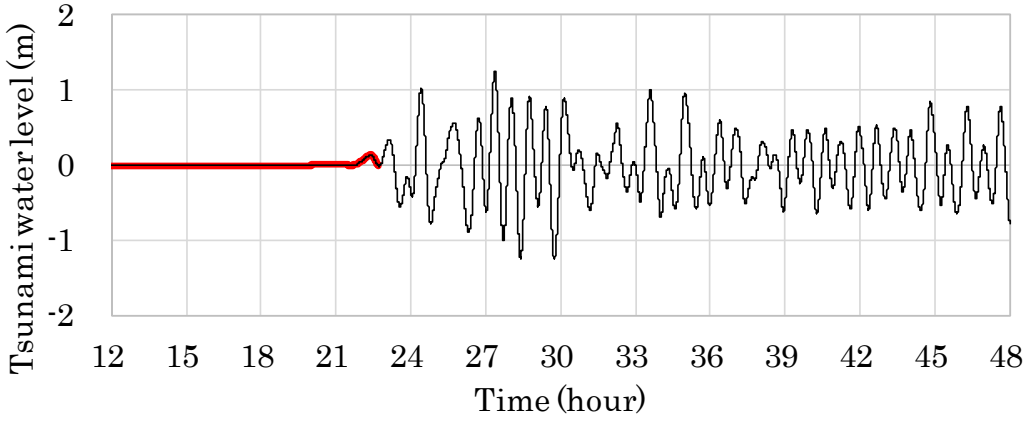

Fig. 7 – Tsunami waveform at Mera, Japan for the 1960 Valdivia earthquake (red line: observation time length [T] of 1,361 minutes after the occurrence of the earthquake including the first arrival)

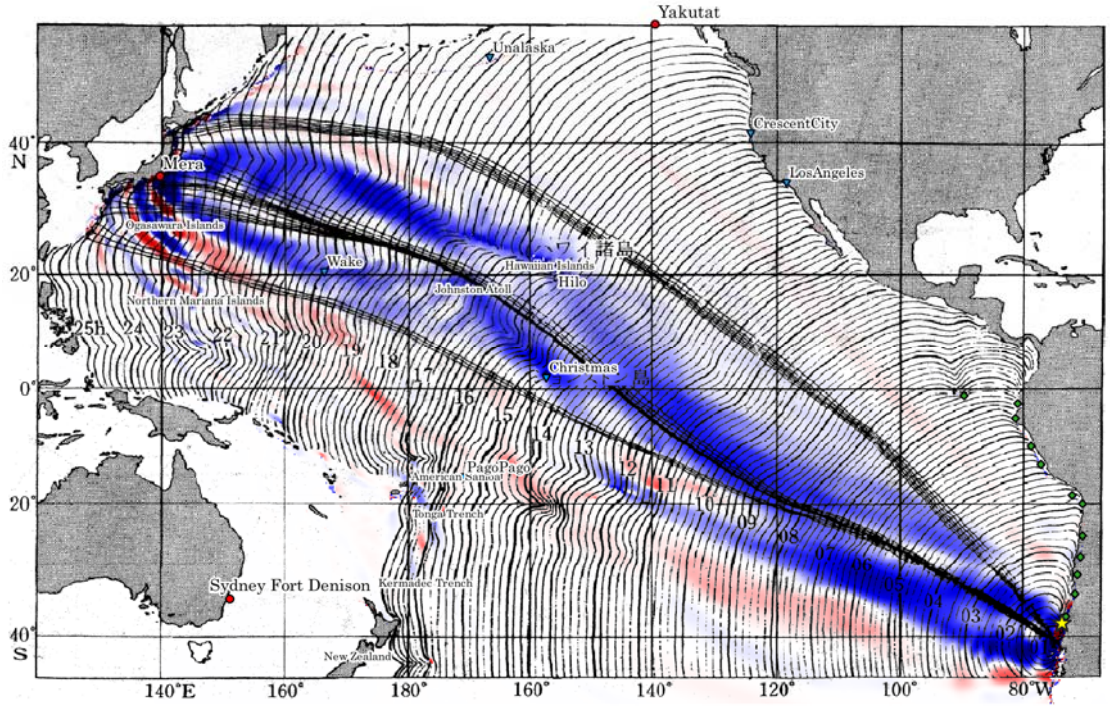

Fig. 8 – Distribution of sensitivity kernel for the tsunami waveforms including the main phase from the coast of Chili to the coast of Japan (contour line). Wave direction by the wave-ray method [11] is shown.

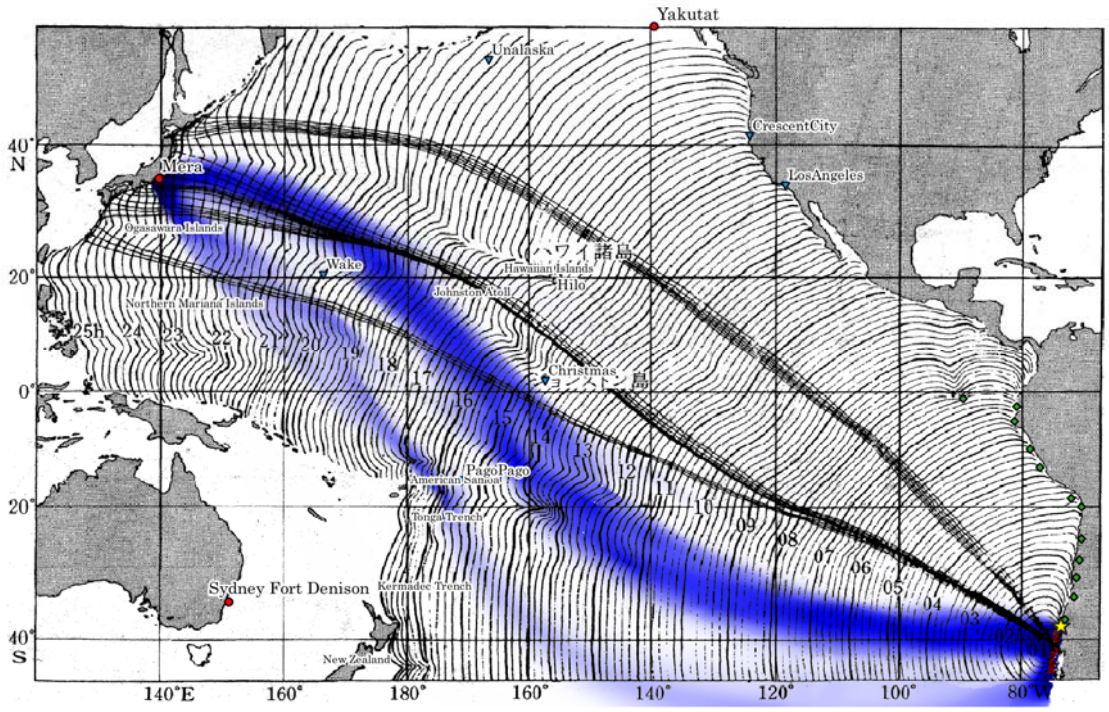

Fig. 9 – Distribution of sensitivity kernel for the tsunami waveforms including the first arrival of tsunami from the coast of Chili to the coast of Japan (contour line). Wave direction by the wave-ray method [11] is shown.

4. Conclusion

In this study, by applying the adjoint method to numerical data from the tsunami simulation for the 1960 Valdivia earthquake, we estimated the sensitivity kernel distributions from the coast of Chili to the coast of Japan in the Pacific Coast. As the results, we obtained the characteristics of the tsunami propagation path for the main phase of tsunami coming from the Hawaiian Islands to the coast of Japan. This result has the same tendency of the result by the wave-ray method in the previous study (Imamura et al., 1990). On the other hand, we obtained the characteristics of the tsunami propagation path for the first arrival of tsunami coming from the south of the Hawaiian Islands to the coast of Japan. Finally, we concluded that this method has a high potential to investigate the tsunami propagation path to the target area.

Acknowledgements

A part of this work is financially supported by the Japanese Ministry of Land, Infrastructure and Transport.

References

[1] Imamura F, Shuto N, Goto C (1990): Study on numerical simulation of the transoceanic propagation of tsunami Part 2: Characteristics of tsunami propagating over the Pacific Ocean. *Zisin 2*, **43**, 389-402. (in Japanese with English abstract)

[2] Tromp J, Tape C, Liu Q (2005): Seismic tomography, adjoint methods, time reversal and banana-doughnut kernels. *Geophys. J. Int.*, **160**, 195-216.

[3] Goto C, Imamura F, Shuto N (1988): Study on numerical simulation of the transoceanic propagation of tsunami Part 1: Governing equation and mesh length. *Zisin 2*, **41**, 515-526. (in Japanese with English abstract)

[4] Inazu D, Saito T (2013): Simulation of distant tsunami propagation with a radial loading deformation effect. *Earth, Planets and Space*, **65**, 835-842.

[5] Watada S, Kusumoto S, Satake K (2014): Traveltime delay and initial phase reversal of distant tsunamis coupled with the self-gravitating elastic Earth. *J. Geophys. Res. Solid Earth*, **119**, 4287-4310.

[6] British Oceanographic Data Centre (1997): The centenary edition of the GEBCO digital atlas (CD-ROM).

[7] Fujii Y, Satake K (2013): Slip distribution and seismic moment of the 2010 and 1960 Chilean earthquakes inferred from tsunami waveforms and coastal geodetic data. *Pure Appl. Geophys*. **170**, 1493-1509.

[8] Barrientos S E, Ward S N (1990): The 1960 Chile earthquake-inversion for slip distribution from surface deformation, *Geophysical Journal International*, **103(3)**, 589–598.

[9] Okada Y (1992): Internal deformation due to shear and tensile faults in a half-space. *Bull. Seismol. Soc. Am.*, **82(2)**, 1018-1040.

[10] Maeda T, Tsushima H, Furumura T (2016): An effective absorbing boundary condition for linear long-wave and linear dispersive-wave tsunami simulations. *Earth, Planets and Space*, 68:63.

[11] Watanabe H (1985): Comprehensive list of tsunamis to hit the Japanese islands. (in Japanese)

